ISSN 1674-1056
http://cpb.iphy.ac.cn
http://iopscience.iop.org/cpb
中国物理 B
Chinese Physics
中国物理 Chinese Physics B

Absorption linewidth inversion with wavelength modulation spectroscopy

Yue Yan(颜悦), Zhenhui Du(杜振辉), Jinyi Li(李金义), Ruixue Wang(王瑞雪)
Citation: Chin. Phys. B . 2018, 27(2): 024205. **doi:** 10.1088/1674-1056/27/2/024205

Journal homepage: http://cpb.iphy.ac.cn; http://iopscience.iop.org/cpb

What follows is a list of articles you may be interested in

Wavelength modulation spectroscopy for measurements of gas parameters in combustion field

Dong-Sheng Qu(屈东胜), Yan-Ji Hong(洪延姬), Guang-Yu Wang(王广宇), Hu Pan(潘虎)
Chin. Phys. B . 2017, 26(6): 064207. **doi:** 10.1088/1674-1056/26/6/064207

Adjustable quantum coherence effects in a hybrid optomechanical system

Wen-Qing Xia(夏文清), Ya-Fei Yu(於亚飞), Zhi-Ming Zhang(张智明)
Chin. Phys. B . 2017, 26(5): 054210. **doi:** 10.1088/1674-1056/26/5/054210

aser absorption spectroscopy

Qin-Bin Huang(黄秦斌), Xue-Mei Xu(许雪梅), Chen-Jing Li(李晨静), Yi-Peng Ding(丁一鹏), Can Cao(曹粲), Lin-Zi Yin(尹林子), Jia-Feng Ding(丁家峰)
Chin. Phys. B . 2016, 25(11): 114202. **doi:** 10.1088/1674-1056/25/11/114202

Spectroscopy system based on a single quantum cascade laser for simultaneous detection of CO and CO_2

Min Wei(魏敏), Qing-Hao Ye(叶擎昊), Rui-Feng Kan(阚瑞峰), Bing Chen(陈兵), Chen-Guang Yang(杨晨光), Zhen-Yu Xu(许振宇), Xiang Chen(陈祥), Jun Ruan(阮俊), Xue-Li Fan(范雪丽), Wei Wang(王薇), Mai Hu(胡迈), Jian-Guo Liu(刘建国)
Chin. Phys. B . 2016, 25(9): 094210. **doi:** 10.1088/1674-1056/25/9/094210

Effect of radiation-induced color centers absorption in optical fibers on fiber optic gyroscope for space application

Jing Jin(金靖), Ya Li(李亚), Zu-Chen Zhang(张祖琛), Chun-Xiao Wu(吴春晓), Ning-Fang Song(宋凝芳)
Chin. Phys. B . 2016, 25(8): 084213. **doi:** 10.1088/1674-1056/25/8/084213

Absorption linewidth inversion with wavelength modulation spectroscopy*

Yue Yan(颜悦)[1], Zhenhui Du(杜振辉)[1,†], Jinyi Li(李金义)[2], and Ruixue Wang(王瑞雪)[1]

[1] State Key Laboratory of Precision Measuring Technology and Instruments, Tianjin University, Tianjin 300072, China
[2] Key Laboratory of Advanced Electrical Engineering and Energy Technology, Tianjin Polytechnic University, Tianjin 300387, China

(Received 2 November 2017; revised manuscript received 30 November 2017; published online 5 January 2018)

For absorption linewidth inversion with wavelength modulation spectroscopy (WMS), an optimized WMS spectral line fitting method was demonstrated to infer absorption linewidth effectively, and the analytical expressions for relationships between Lorentzian linewidth and the separations of first harmonic peak-to-valley and second harmonic zero-crossing were deduced. The transition of CO_2 centered at 4991.25 cm^{-1} was used to verify the optimized spectral fitting method and the analytical expressions. Results showed that the optimized spectra fitting method was able to infer absorption accurately and compute more than 10 times faster than the commonly used numerical fitting procedure. The second harmonic zero-crossing separation method calculated an even 6 orders faster than the spectra fitting without losing any accuracy for Lorentzian dominated cases. Additionally, linewidth calculated through second harmonic zero-crossing was preferred for much smaller error than the first harmonic peak-to-valley separation method. The presented analytical expressions can also be used in on-line optical sensing applications, electron paramagnetic resonance, and further theoretical characterization of absorption lineshape.

Keywords: absorption linewidth, wavelength modulation spectroscopy, absorption spectroscopy, spectral line fitting, separation of harmonics

PACS: 42.60.Fc, 42.68.Ca, 42.79.–e **DOI:** 10.1088/1674-1056/27/2/024205

1. Introduction

Spectral linewidth is an important parameter in electron paramagnetic resonance (EPR),[1] nuclear magnetic resonance (NMR)[2] as well as molecular absorption spectroscopy.[3] The accurate measurement of absorption linewidth is conducive to the analysis of spectral properties, for example, determination of the intermolecular collisional coefficient depends on the accurate measurement of the linewidth.[4] In wavelength modulation spectroscopy (WMS), fast and accurate linewidth determination can be used to correct the measurement errors of gas concentration and (or) temperature due to linewidth broadening in real time.[5,6] Therefore, it is essential to rapidly and accurately measure the absorption linewidth.

Measurements of absorption linewidth have received a great deal of attention.[7–10] In optical spectroscopy, the absorption linewidth can be obtained directly by spectrum measurement, but the accuracy of this method is limited by the low resolution of the spectrometer and small absorbance of the target spectrum. Practically, the absorption linewidth can be derived by nonlinear least squares fitting of the direct absorption spectrum (DAS) signal, which is also used to measure the intermolecular collisional coefficient under laboratory conditions.[11–13] However, the measurement accuracy is often restricted by baseline fluctuation and lower absorbance. Wavelength modulation spectroscopy has been developed to meet lower absorbance.[14–17] The absolute gas absorption lineshape can be recovered from wavelength modulation by using the phasor decomposition method (PDM), however, it is more costly as it requires more sophisticated RF lock-in equipment.[18,19] Absorption linewidth can also be obtained by nonlinear least squares fitting of the complete harmonic signals,[20,21] which is also applicable for overlap lines cases. However, the traditional numerical process of simulating the harmonic signals is quite time consuming. Researchers have also proposed to retrieve the Lorentzian linewidth from the separation of the first or second harmonic signals,[8–10] which can infer the absorption linewidth more rapidly. However, at present, these methods are all numerical computations without any analytical solution.

In this paper, an optimized WMS spectral fitting method was demonstrated to calculate the absorption linewidth effectively, and the analytical expressions for relationships between Lorentzian linewidth and the separation of first harmonic peak-to-valley, and second harmonic zero-crossing were derived to infer the absorption linewidth much more rapidly. The transition of CO_2 centered at 4991.25 cm^{-1} was used to verify the presented spectral fitting method and the analytical expressions.

*Project supported by the National Natural Science Foundation of China (Grant No. 61505142) and the Tianjin Natural Science Foundation (Grant No. 16JCQNJC02100).

†Corresponding author. E-mail: duzhenhui@tju.edu.cn

© 2018 Chinese Physical Society and IOP Publishing Ltd

2. Theory

2.1. Linewidth inversion with WMS spectral fitting

Wavelength modulation spectroscopy is a widely used technique,[22,23] and the second harmonic signal is also commonly used for the measurement of lineshape parameters.[24] Linewidth of the gas absorption spectrum can be derived by fitting the complete second harmonic signal.

For optically thin conditions (absorbance $\alpha(v) = A\varphi(v) < 0.1$), the demodulated k-th harmonic signals can be expressed as:

$$H_k(v) = -\frac{A}{\pi}\int_{-\pi}^{\pi}\varphi_{\mathrm{V}}(\bar{\nu}+a\cos\theta,\Delta\nu_{\mathrm{L}},\Delta\nu_{\mathrm{G}})\cos k\theta\,\mathrm{d}\theta,\quad k>0, \tag{1}$$

where A is the integral absorbance, $\varphi(v)$ is the absorption lineshape which is generally described as the Voigt lineshape. a is the modulation amplitude, and modulation index $m = a/\Delta\nu_{\mathrm{V}}$ determines the lineshapes and amplitudes of the k-harmonic waves. $\Delta\nu_{\mathrm{V}}$, $\Delta\nu_{\mathrm{L}}$, and $\Delta\nu_{\mathrm{G}}$ are the half width at half maximum (HWHM) of Voigt, Lorentzian, and Gaussian linewidths, respectively.

Then the second harmonic $H_2(v)$ signal can be simulated according to Eq. (1), which was used to fit with the measured $H_2(v)$ signal to infer the absorption linewidth. However, equation (1) has no analytical solution and it can be evaluated only numerically which is complex and time consuming.

To optimize the fitting procedure, Voigt profile φ_{V} was approximated with the following weighted combination of Lorentzian φ_{L} and Gaussian φ_{G} functions[25]

$$\varphi_{\mathrm{V}}(v-v_0,\Delta\nu_{\mathrm{V}}) \approx c_{\mathrm{L}}\frac{1}{\pi}\frac{\Delta\nu_{\mathrm{V}}}{(v-v_0)^2+\Delta\nu_{\mathrm{V}^2}} + c_{\mathrm{G}}\frac{\sqrt{\ln 2}}{\sqrt{\pi}\Delta\nu_{\mathrm{V}}} \times \exp\left[-\ln 2\left(\frac{v-v_0}{\Delta\nu_{\mathrm{V}}}\right)^2\right], \tag{2}$$

where c_{L} and c_{G} are weighted Lorentzian and Gaussian coefficients respectively, $\Delta\nu_{\mathrm{V}}$ is the Voigt broadening width which can be calculated by[26]

$$\Delta\nu_{\mathrm{V}} = 0.5\cdot(1.0692\Delta\nu_{\mathrm{L}} + \sqrt{0.86639\Delta\nu_{\mathrm{L}}^2 + 4\Delta\nu_{\mathrm{G}}^2}). \tag{3}$$

Then the k-th harmonic signals of Voigt profile H_k can be expressed as[27]

$$H_k \approx c_{\mathrm{L}}\cdot H_{\mathrm{L},k} + c_{\mathrm{G}}\cdot H_{\mathrm{G},k}, \tag{4}$$

where $H_{\mathrm{L},k}$ and $H_{\mathrm{G},k}$ are the k-th harmonic signals of Lorentzian and Gaussian profiles respectively, which were explicitly expressed by Kluczynski *et al.*[28,29] Therefore, equation (4) was then substituted by the linear combination Eq. (1) in order to simulate the $H_2(v)$ signal more effectively, thus accelerating the spectral fitting procedure.

Levenberg–Marquardt (LM) algorithm is used as the fitting method. The center wavenumber v_0, the integral absorbance A, the Lorentzian linewidth $\Delta\nu_{\mathrm{L}}$ and Gaussian linewidth $\Delta\nu_{\mathrm{G}}$ are participated in the fitting procedure as free parameters. The simulated $H_2(v)$ signal obtained with Eq. (4) then was fitted to the measured $H_2(v)$ signal through nonlinear iterating until the best fitted parameters were produced. The fitting flow chart is shown in Fig. 1.

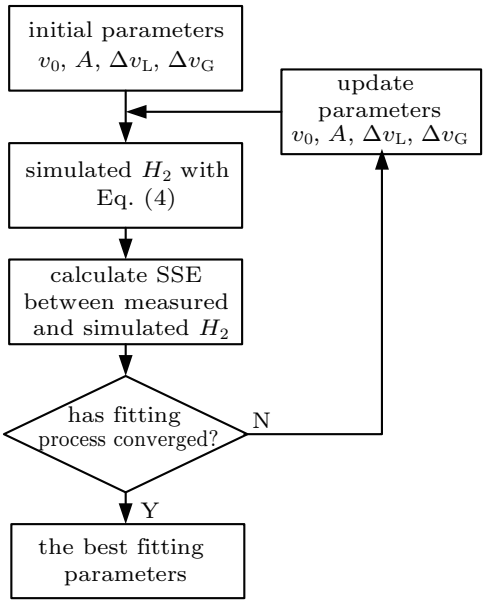


Fig. 1. Flow chart of the fitting procedure.

The optimized WMS spectral fitting procedure was able to extract the absorption linewidth more effectively. However, in some faster measurement occasions, the computing time should be improved further. It can be demonstrated that the absorption linewidth was able to be inferred from the separations of harmonic signals much faster than the fitting method.

2.2. Linewidth inversion with separations of 1st and 2nd harmonics

It is known that the larger the separations of harmonic signals are, the wider the absorption linewidth will be. The absorption linewidth can be well inferred from the peak-to-valley separation of the first harmonic signal $H_1(v)$ and the zero-crossing separation of the second harmonic signal $H_2(v)$.

When collisional broadening was dominated, the absorption lineshape $\varphi(v)$ can be well described as Lorentzian function, the normalized Lorentzian lineshape $L(v)$ can be expressed as:

$$L(v) = \frac{1}{\pi}\frac{\Delta\nu_{\mathrm{L}}}{\Delta\nu_{\mathrm{L}}^2+(v-v_0)^2}. \tag{5}$$

The modulated Lorentzian lineshape then can be expressed as

$$L[v(t)] = \frac{1}{\pi}\frac{\Delta\nu_{\mathrm{L}}}{\Delta\nu_{\mathrm{L}}^2+(\bar{\nu}+a\cos wt-v_0)^2}, \tag{6}$$

then equation (1) can be expressed as:

$$H_k = \frac{A}{\pi}\int_{-\pi}^{\pi} \frac{\cos k\theta}{\Delta v_{\rm L}^2 + (\bar{v} + a\cos\theta - v_0)^2}\,{\rm d}\theta. \tag{7}$$

Define:

$$\alpha = \frac{v - v_0}{a}, \quad \beta = \frac{\Delta v_{\rm L}}{a}, \tag{8}$$

$$r = 1 + \alpha^2 + \beta^2, \quad u = r + [r^2 - 4\alpha^2]^{1/2}. \tag{9}$$

In the cases of $k = 1$, 2, the first harmonic signal $H_1(v)$ and the second harmonic signal $H_2(v)$ can be expressed as:[30]

$$H_1 = \pm A \cdot \left(\frac{2}{a}\right)^2 \left[\frac{(2r-u)^{1/2}}{2(u-2)^{1/2}(u-r)}\right], \tag{10}$$

$$H_2 = -A \cdot \left(\frac{2}{a}\right)^2 \left[1 + \frac{u^{1/2}(1+2r-2u)}{2(u-2)^{1/2}(u-r)}\right]. \tag{11}$$

According to the properties of $H_1(v)$ and $H_2(v)$ signals, the analytical expressions of relationships between linewidth $\Delta v_{\rm L}$ and the $H_1(v)$ peak-to-valley separation $\Delta w_{\rm p}$ ($H_2(v)$ zero-crossing separation $\Delta w_{\rm z}$) are deduced as follows:

(i) Setting ${\rm d}H_1/{\rm d}v = 0$, the solution then can be obtained as:

$$\beta = \sqrt{\frac{3[(4\alpha_{\rm p}^2 - \sqrt{16\alpha_{\rm p}^4 - 12\alpha_{\rm p}^2}) - 2]^2}{4[2(4\alpha_{\rm p}^2 - \sqrt{16\alpha_{\rm p}^4 - 12\alpha_{\rm p}^2}) - 3]}}, \quad 0 < \beta < \frac{1}{2},$$

$$\beta = \sqrt{\frac{3[(4\alpha_{\rm p}^2 + \sqrt{16\alpha_{\rm p}^4 - 12\alpha_{p}^2}) - 2]^2}{4[2(4\alpha_{\rm p}^2 + \sqrt{16\alpha_{\rm p}^4 - 12\alpha_{\rm p}^2}) - 3]}}, \quad \beta > \frac{1}{2}, \tag{12}$$

where $\alpha_{\rm p}$ represents the α value at the extreme positions of the $H_1(v)$ signal, $|\alpha_{\rm p}| = \Delta w_{\rm p}/2a$, when $\beta = (\Delta v_{\rm L}/a) = 1/2$, $\alpha_{\rm p}^2 = 3/4$.

(ii) Setting $H_2(v) = 0$, the solution can then be obtained as:

$$\beta = f(\alpha_z) = \frac{\sqrt{3}}{3}\sqrt{\alpha_z^2 + 2\sqrt{16\alpha_z^4 + 12\alpha_z^2}\cdot\cos\left(\theta - \frac{\pi}{3}\right) - 3},$$

$$\beta \geq \sqrt{\frac{5}{64}},$$

$$\theta = \frac{\arccos T}{3}, \quad T = \frac{-512\alpha_z^6 + 1152\alpha_z^4 + 27\alpha_z^2}{8(16\alpha_z^4 + 12\alpha_z^2)^{3/2}}, \tag{13}$$

where α_z represents the α value at the zero-crossing positions of the $H_2(v)$ signal, $|\alpha_{\rm p}| = \Delta w_{\rm z}/2a$, when $\beta = (\Delta v_{\rm L}/a) = \sqrt{5/64}$, $\alpha_{\rm p}^2 = \sqrt{27/64}$.

The first harmonic $H_1(v)$ and the second harmonic $H_2(v)$ were simulated by using Eq. (10) and Eq. (11), as shown in Figs. 2(a) and 2(b), respectively. It can be seen that different absorption linewidths $\Delta v_{\rm L}$ correspond to different $H_1(v)$ peak-to-valley separation $\Delta w_{\rm p}$ and different $H_2(v)$ zero-crossing separation $\Delta w_{\rm z}$. As modulation depth a is fixed, absorption linewidth $\Delta v_{\rm L}$ can be inferred from both the $\Delta w_{\rm p}$ and $\Delta w_{\rm z}$ according to Eq. (12) and Eq. (13) respectively.

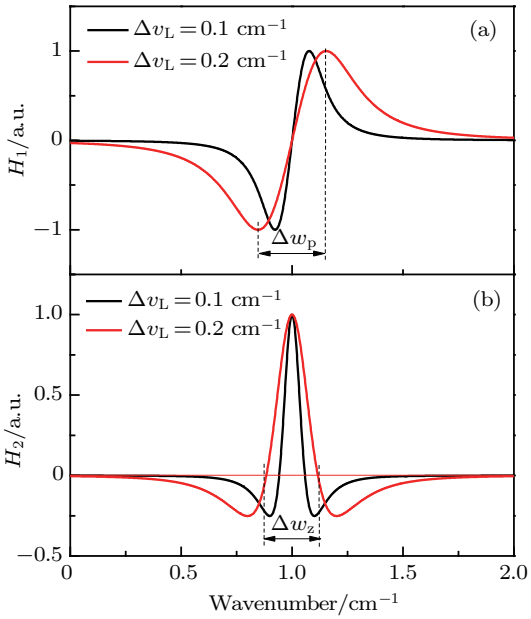


Fig. 2. (color online) (a) The simulated first harmonic, $\beta = (\Delta v_{\rm L}/a) = 1.45$, $\Delta w_{\rm p}$ is the $H_1(v)$ peak-to-valley separation, when $\Delta w_{\rm p} = 0.153$ cm^{-1}, $\Delta v_{\rm L} = 0.1$ cm^{-1}; when $\Delta w_{\rm p} = 0.307$ cm^{-1}, $\Delta v_{\rm L} = 0.2$ cm^{-1}; (b) the simulated second harmonic, $\beta = (\Delta v_{\rm L}/a) = 0.88$, $\Delta w_{\rm z}$ is the $H_2(v)$ zero-crossing separation, when $\Delta w_{\rm z} = 0.177$ cm^{-1}, $\Delta v_{\rm L} = 0.1$ cm^{-1}; when $\Delta w_{\rm z} = 0.354$ cm^{-1}, $\Delta v_{\rm L} = 0.2$ cm^{-1}, the signal amplitudes were normalized.

Both $\Delta w_{\rm p}$ and $\Delta w_{\rm z}$ are collectively referred to as Δw, the accuracy with which one can infer $\Delta v_{\rm L}$ from Δw depends upon both the detection sensitivity and the amplitudes of the first or second harmonic signal. The relationships between $\beta(\Delta v_{\rm L}/a)$ and $\Delta w/a$ were obtained according to Eq. (11) and Eq. (12) (Fig. 3(a)), and define $|{\rm d}(\Delta w/a)/{\rm d}\beta|$ as the detection sensitivity S (Fig. 3(b)). The maximal amplitude of the first and the second signals were collectively referred to as $A_{\rm max}(\beta)$, the relationships between $A_{\rm max}(\beta)$ and β are shown in Fig. 3(c).[31,32] As shown in Figs. 3(b) and 3(c), the detection sensitivity S has a big value for big β, while the signal amplitude $A_{\rm max}(\beta)$ has a small value for big β. Therefore, a guideline was introduced to help choose a compromise modulation amplitude for the combination of signal amplitudes and sensitivity.

Let C be equal to the product of $S(\beta)$ and $A_{\rm max}(\beta)$:

$$C(\beta) = S(\beta)\cdot A_{\rm max}(\beta). \tag{14}$$

The parameter C is considered to be a guideline that helps to choose a compromise modulation amplitude for the combination of signal amplitudes and sensitivity. When C reaches its maximum, the corresponding β value will be chosen as the optimal value. By using Eq. (14), it can be observed that the $C(\beta)$ function is maximized at $\beta = 1.45$ and 0.88 ($m = 0.69$ and 1.14) when applying $H_1(v)$ peak-to-valley and $H_2(v)$ zero-crossing separation to infer absorption linewidth respectively (Fig. 3(d)). It should also be noted that the absorption linewidth to be measured is unknown beforehand, which

is common in practical situations. So it is impossible to set the optimal modulation index accurately, and the optimum values obtained from Fig. 3(d) were for reference only.

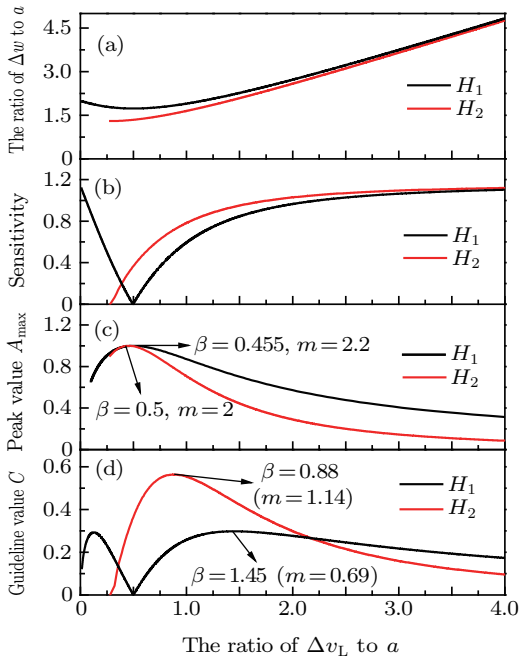


Fig. 3. (color online) (a) The relationships between the ratio of absorption linewidth to modulation depth ($\Delta\nu_L/a$) and the ratio of $\Delta w/a$; (b) the relationships between ($\Delta\nu_L/a$) and sensitivity; (c) the relationships between ($\Delta\nu_L/a$) and the peak value $A_{max}(\beta)$; (d) the relationships between ($\Delta\nu_L/a$) and the guide value C.

3. Experiment

The absorption spectrum of CO_2 centered at 4991.25 cm^{-1} was selected as the target spectrum to verify the WMS spectral line fitting method and analytical expressions demonstrated in Section 2.

The experimental setup is constructed based on tunable laser absorption spectroscopy with an NIR-infrared laser, a laser controller, an amplified detector, a homemade digital lock-in amplifier (DLIA), an embedded processor, an F–P etalon and a white cell, as shown in Fig. 4. The laser, from Nanoplus Germany, is a butterfly packaged distributed feedback laser (DFB) with central wavelength of 2004 nm and current tuning rate of 0.045 cm^{-1}/mA. The laser's injection current and temperature are controlled by the laser controller (ILX Lightwave, LDC-3908) with current noise of 10 μA rms and temperature stability of ±0.01 °C. The F–P etalon is used to monitor the laser wavelength. The DLIA is used to demodulate the first and second harmonics.[33]

The laser frequency of the scanning range was linearized by using the F–P etalon (FSR = 1.5 GHz). The laser injection current scanned from 75 mA to 105 mA with a 10-Hz repetitive ramp ride with a 2-kHz sinusoid. The laser working temperature is 33.9 °C. The filter parameters of the DLIA were set to 10 ms and 18 dB/oct, respectively. The ambient air is filled to the white cell used as target gas. Before experiment, the optical configuration was carefully adjusted, including the laser incidence and the field mirror inside the white cell, to ensure excellent experiment conditions. The path-length of the white cell is set to 10 meters, which is directly measured by using an optical frequency domain reflectometer with relative uncertainty of 10^{-6}.[34]

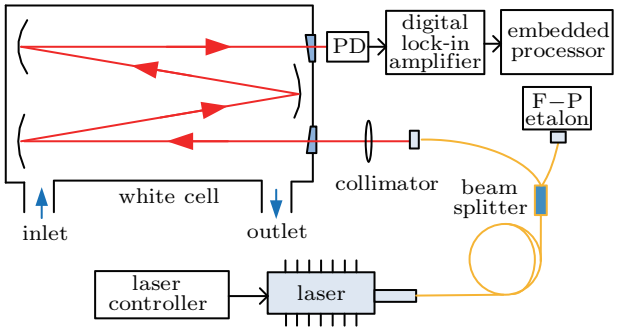


Fig. 4. (color online) Schematic diagram of the overall experimental setup.

4. Results

First, the absorption linewidth of the target spectrum was derived by fitting the measured $H_2(v)$ signal with LM algorithm. Set three initial parameters: v_0, A, and $\Delta\nu_L$ as free parameters, $\Delta\nu_G$ was set as a constant (0.0046 cm^{-1}) corresponding to T = 296 K. The best-fitted parameter $\Delta\nu_L$ = 0.0762 cm^{-1} was derived after 126 nonlinear iterations according to the procedure as shown in Fig. 1. The fitting results are shown in Fig. 5. Then the absorption linewidth (Voigt) was calculated to be 0.0766 cm^{-1}.

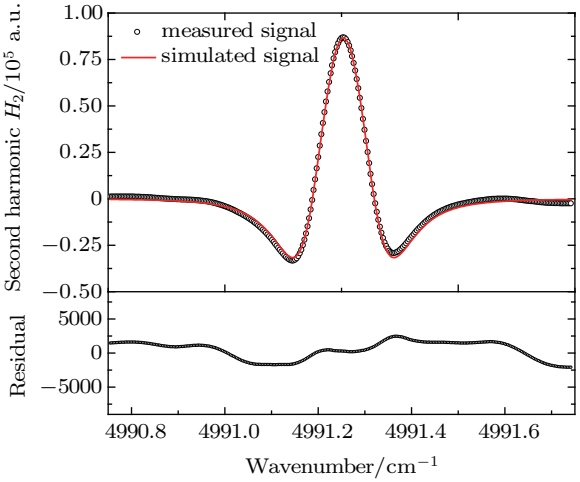


Fig. 5. (color online) The measured and simulated $H_2(v)$ signals, modulation depth a = 0.084 cm^{-1}, the best fitted parameters $\Delta\nu_L$ = 0.0762 cm^{-1}, and Voigt linewidth was calculated to be 0.0766 cm^{-1}. The unit a.u. is short for arbitrary units.

By approximately calculating the Voigt profile with the weighted combination of Lorentzian and Gaussian functions, the $H_2(v)$ signal can be simulated quickly and accurately, thus

greatly decreasing the calculation time of the fitting algorithm. In fact, for a processor configured as Intel(R) Core(TM) i5-4590 CPU@3.30 GHz, the fitting procedure needed about 1.7 s of calculation time compared with the 22 s needed in the case of the traditional numerical fitting method reported in Subsection 2.1. The absorption linewidth can also be inferred even much faster through $H_1(v)$ peak-to-valley or $H_2(v)$ zero-crossing separation.

The ratio of the Lorentzian linewidth to the Doppler linewidth of the target spectrum was calculated to be $0.0762/0.0046 \approx 16.5$. So the target spectrum can be well described as a Lorentzian lineshape. On the basis of the analysis in Subsection 2.2, considering both the measurement sensitivity and SNR, the modulation depths were estimated and set to be 0.051 cm^{-1} and 0.084 cm^{-1} (corresponding to the sinusoidal current amplitudes of 1.65 mA and 2.72 mA) for applying $H_1(v)$ peak-to-valley and $H_2(v)$ zero-crossing separation to infer absorption linewidth, respectively. The measured $H_1(v)$ and $H_2(v)$ signals are shown in Figs. 6(a) and 6(b) respectively. As shown in Fig. 6, the peak-to-valley separation of the $H_1(v)$ signal was located at $\Delta w_p = 0.119$ cm^{-1}, absorption linewidth was calculated by using Eq. (12) to be $\Delta v_L = 0.0802$ cm^{-1}; the zero-crossing separation of the $H_2(v)$ signal was located at $\Delta w_z = 0.132$ cm^{-1}, absorption linewidth then was calculated by using Eq. (13) to be $\Delta v_L = 0.0755$ cm^{-1}.

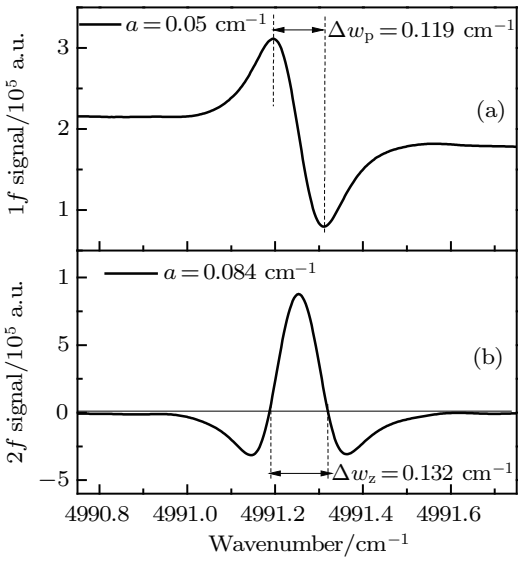


Fig. 6. (color online) (a) $H_1(v)$ signal of the target CO_2 absorption, the modulation depth $a = 0.051$ cm^{-1}, peak to valley separation $\Delta w_p = 0.119$ cm^{-1}, the inferred absorption linewidth was 0.0802 cm^{-1}; (b) $H_2(v)$ signal of the target CO_2 absorption, the modulation depth $a = 0.084$ cm^{-1}, zero-crossing separation $\Delta w_z = 0.132$ cm^{-1}, the inferred absorption linewidth was 0.0755 cm^{-1}.

The $H_1(v)$ and $H_2(v)$ signals were continuously collected and the corresponding absorption linewidth were inferred from three different methods: WMS spectral line fitting, $H_1(v)$ peak-to-valley separation, $H_2(v)$ zero-crossing separation. The results are shown in Fig. 7 and Table 1. All of the above results were compared with the result from the HITRAN database which was regarded as the true value.

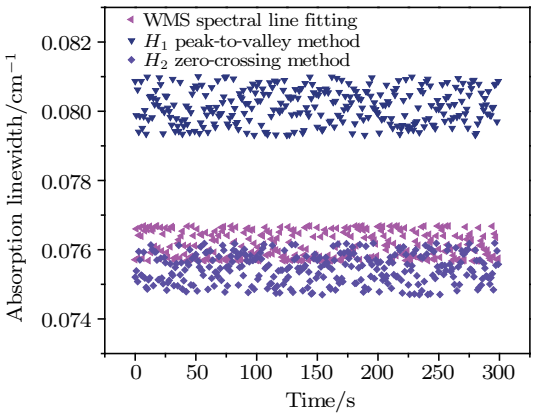


Fig. 7. (color online) Absorption linewidth results inferred from the WMS spectral line fitting, $H_1(v)$ peak-to-valley separation and $H_2(v)$ zero-crossing separation respectively with 1-s time interval.

Table 1. Results inferred from the WMS spectral line fitting, $H_1(v)$ peak-to-valley separation and $H_2(v)$ zero-crossing separation respectively.

Methods	Absorption linewidth/cm^{-1}	Relatively error/%	Uncertainty/ 3σ/%[a]
Hitran database[35]	0.0738	–	–
WMS spectral fitting	0.0761	3.1	1.5
$H_1(v)$ peak-to-valley	0.0801	8.5	2.0
$H_2(v)$ zero-crossing	0.0754	2.2	1.7

[a] σ is the measured standard deviation

From Table 1, we can see that the absorption linewidths obtained by the presented $H_2(v)$ zero-crossing separation and WMS spectral line fitting were very close to the figures simulated by the HITRAN database. We can also see from Table 1 that the WMS fitting method shows the smallest measurement uncertainty, which possesses a better immunity of noise, since the fitting procedures have taken both the whole Lorentzian and Doppler lineshapes into consideration. In addition, the WMS spectra fitting method was also suitable for spectral overlapping cases.

It has been demonstrated that the WMS fitting procedure was much optimized by replacing Eq. (1) with Eq. (4). However, it still needs 1.7 s to complete one single linewidth measurement, which can hardly meet many high time resolved requirements. Compared with the WMS spectral fitting method, for the same processor, the computing time with the $H_1(v)$ peak-to-valley or $H_2(v)$ zero-crossing separation method was less than 0.43 μs which is 6 orders faster and can be negligible in almost all applications.

In addition, as shown in Table 1, the relative errors of the measured absorption linewidth by the presented $H_1(v)$ peak-to-valley or $H_2(v)$ zero-crossing separation method are 8.5% and 2.2% respectively. It is not surprising that the $H_2(v)$ zero-crossing separation method is more accurate than the $H_1(v)$ peak-to-valley separation method. The $H_1(v)$ peak-to-valley

separation method relies upon the positions of peak and valley of the $H_1(v)$ signal whose slope is parallel to the x axis, however, the zero-crossing positions of the $H_2(v)$ signal are very steep, which leads to a higher signal to noise ratio and more accurate measurement. Because of the geographical differences, the air composition deviation exists between our laboratory and the air USA model in the HITRAN database, resulting in some deviation between the measured results and the figure from the HITRAN database. Besides, the error of the modulation depth a, the electromagnetic noise, and optical fringes of the experimental system could also attribute to the measurement error. Moreover, it should be pointed out that the analytical expressions for relationships between Lorentzian linewidth and the separations of first and second harmonics established in this paper are only suitable for spectrum that can be well described as Lorentzian lineshape, the presented WMS spectral fitting method is still recommended if both Lorentzian and Doppler linewidth are comparable.

5. Conclusion

In this paper, three methods for inferring absorption linewidth were presented: WMS spectral line fitting, peak-to-valley separation of first harmonic, and zero-crossing separation of second harmonic. The spectral fitting procedure was optimized by calculating the Voigt profile with the weighted combination of Lorentzian and Gaussian functions, which largely decreased the computing time. In order to meet the high time resolution required in applications, the analytical expressions for relationships between Lorentzian linewidth and the separations of 1st harmonic peak-to-valley and 2nd harmonic zero-crossing were deduced, which computing speed is 6 orders faster than the spectral fitting method. To the best of our knowledge, the $H_2(v)$ zero-crossing method performed better than the $H_1(v)$ peak-to-valley method. When both Lorentzian and Doppler linewidth are non-negligible, the optimized spectral fitting is still recommended as the preference.

References

[1] Deng Y, Pandian R P, Ahmad R, Kuppusamy P and Zweier J L 2006 *J. Magn. Reson.* **181** 254
[2] Kaplan J I and Vasavada K V 1983 *J. Magn. Reson.* **52** 475
[3] Eng R S and Mantz A W 1979 *J. Mol. Spectrosc.* **74** 331
[4] Daneshvar L, F?ldes T, Buldyreva J and Auwera J V 2014 *J. Quantum Spectrosc. Radiat. Transfer* **149** 258
[5] Linnerud I, Kaspersen P and Jaeger T 1998 *Appl. Phys. B* **67** 297
[6] Rieker G B, Jeffries J B and Hanson R K 2009 *Appl. Opt.* **48** 5546
[7] Vreede J P M D, Mehrotra S C, Tal A and Dijkerman H A 1982 *Appl. Spectrosc.* **36** 227
[8] Reeves G K and Wilson G V H 1970 *J. Phys. D: Appl. Phys.* **3** 1609
[9] Smith G W 1964 *J. Appl. Phys.* **35** 1217
[10] Proffitt M H and Jr W C G 1977 *J. Magn. Reson.* **25** 423
[11] Lepère M, Henry A, Valentin A and Camy-Peyret C 2001 *J. Mol. Spectrosc.* **208** 25
[12] Owen K, Essebbar E and Farooq A 2013 *J. Quantum Spectrosc. Radiat. Transfer* **121** 56
[13] Werhahn O 2014 *Mol. Phys.* **112** 2451
[14] Du Z H, Zhen W M, Zhang Z Y, Li J Y and Gao N 2016 *Appl. Phys. B* **122** 100
[15] Xiong B, Du Z H and Li J Y 2015 *Rev. Sci. Instrum.* **86** 113104
[16] Che L, Ding Y J, Peng Z M, and Li X H 2012 *Chin. Phys. B* **21** 127803
[17] Wei M, Ye Q H, Kan R F, *et al.* 2016 *Chin. Phys. B* **25** 094210
[18] Stewart G, Johnstone W, Bain J R P, Ruxton K and Duffin K 2011 *J. Lightw. Technol.* **29** 811
[19] Bain J R P, Johnstone W, Ruxton K, Stewart G, Lengden M and Duffin K 2011 *J. Lightw. Technol.* **29** 987
[20] Setzer B J and Pickett H M 1977 *J. Chem. Phys.* **67** 340
[21] Goldenstein C S, Strand C L, Schultz I A, Sun K, Jeffries J B and Hanson R K 2014 *Appl. Opt.* **53** 356
[22] Supplee J M, Whittaker E A and Lenth W 1994 *Appl. Opt.* **33** 6294
[23] Philippe L C and Hanson R K 1993 *Appl. Opt.* **32** 6090
[24] Li H, Rieker G B, Liu X, Jeffries J B and Hanson R K 2006 *Appl. Opt.* **45** 1052
[25] Liu Y, Lin J, Huang G, Guo Y and Duan C 2001 *J. Opt. Soc. Am. B* **18** 666
[26] Olivero J J and Longbothum R L 1977 *J. Quantum Spectrosc. Radiat. Transfer* **17** 233
[27] Tommasi E D, Castrillo A, Casa G and Gianfrani L 2008 *J. Quantum Spectrosc. Radiat. Transfer* **109** 168
[28] Axner O, Kluczynski P and Lindberg Åsa 2001 *J. Quantum Spectrosc. Radiat. Transfer* **68** 299
[29] Kluczynski P, Lindberg Åsa M and Axner O 2004 *J. Quantum Spectrosc. Radiat. Transfer* **83** 345
[30] Wahlquist H 1961 *J. Chem. Phys.* **35** 1708
[31] Arndt R 1965 *J. Appl. Phys.* **36** 2522
[32] Reid J and Labrie D 1981 *Appl. Phys. B* **26** 203
[33] Du Z H, Zhang Z Y, Zhen W M, Xiong B and Li J Y 2015 *J. Atmos. Environ. Opt.* **10** 165
[34] Du Z H, Gao H and Cao X H 2016 *Opt. Express* **24** 417
[35] Toth R A, Brown L R, Miller C E, Devi V M and Benner D C 2008 *J. Quantum Spectrosc. Radiat. Transfer* **109** 906